Multiuser Receivers for Randomly Spread Signals: Fundamental Limits With and Without Decision-Feedback

Ralf R. Müller, *Associate Member, IEEE*

***Abstract*—Synchronous code-division multiple-access (CDMA) communication systems with randomly chosen spreading sequences and capacity-achieving forward error correction coding are analyzed in terms of spectral efficiency. Emphasis is on the penalties paid by applying single-user coding in conjunction with suboptimal multiuser receivers as opposed to optimal joint decoding which involves complexity that is exponential in the number of users times the codeword length.**

The conventional, the decorrelating, and the (re-encoded) decorrelating decision-feedback detectors are analyzed in the nonasymptotic case for spherical random sequences. The re-encoded minimum mean-squared error (MMSE) decision-feedback receiver achieving the same performance as joint multiuser decoding for equal power users is shown to be suboptimal in the case of equal rates.

***Index Terms*—Decision feedback, decorrelation, information rates, multiaccess communication, spectral efficiency, spherical sequences.**

I. Introduction

In THIS paper, the performances of linear and decision-feedback multiuser receivers using single-user channel coding are analyzed and compared by deriving their position in the power-bandwidth plane for random sequences. This does not only give insight into the crossover points between performances of various receivers, but also facilitates the optimization of both the coding spreading tradeoff and the system load.

Code-division multiple access (CDMA) with random spreading and multiuser receivers was addressed by Madhow and Honig [1] (see also [2]) for the first time and bounds on the signal-to-interference-and-noise ratio (SINR) were found. Later, random sequence multisets for CDMA were discussed by Grant and Alexander [3] (see also [4]). Spectral efficiency of the decorrelator and the statistics of its SINR were then calculated for spherical random sequences in an early conference version of the present paper [5]. Finally, Verdú and Shamai [6] (see also [7]) used random matrix theory to give new asymptotic results on the spectral efficiencies of several linear multiuser receivers and the optimum joint decoder for binary random spreading. At the same time, Tse and Hanly [8] (see also [9]) independently presented new asymptotic results on the SINR of linear multiuser receivers that hold for arbitrary power assignments to the users. In addition to [5] and the other references mentioned in this paragraph, the present paper also extends to decision-feedback receivers and gives nonasymptotic results on spectral efficiency for the spherical random sequence model.

In Sections II–IV, the decorrelating, conventional, and decorrelating decision-feedback multiuser receivers are analyzed for a finite number of users K and a finite spreading factor L under a spherical random sequence model for signaling over the synchronous Gaussian CDMA channel described by

$$\boldsymbol{y} = \boldsymbol{S}^H \boldsymbol{S}\boldsymbol{b} + \boldsymbol{S}^H \boldsymbol{n}.$$

In this channel model $\boldsymbol{S}$, $\boldsymbol{y}$, $\boldsymbol{b}$, $\boldsymbol{n}$ denote the $L \times K$ matrix of signature sequences, the $K \times 1$ vector of matched filter outputs, the $K \times 1$ vector of information bearing symbols, and the $L \times 1$ vector of independent additive white Gaussian noise (AWGN) samples with zero mean, respectively. Section V compares the results found in Sections II–IV with results for other linear and decision-feedback detectors that are asymptotic in the number of users and points out the conclusions.

Throughout this work each spreading sequence, $\boldsymbol{s}$ is modeled by an L-dimensional complex Gaussian random vector $[g_1, g_2, \ldots, g_L]^T$ which is normalized to unit Euclidean norm with L denoting the spreading factor

$$\boldsymbol{s} = \frac{[g_1, g_2, \ldots, g_L]^T}{\sqrt{\sum_{i=1}^{L} |g_i|^2}}. \tag{1}$$

Hereby, the random variables g_i, $1 \le i \le L$, are assumed to be independent zero-mean complex Gaussian distributed variables with equal variance. Since the spreading vectors $\boldsymbol{s}$ are uniformly distributed on the $(L-1)$-dimensional surface of an L-dimensional sphere, this model is called the spherical random sequence model [10]. Note that the spherical random sequence model is different from Gaussian random spreading. Gaussian random spreading was analyzed in context of antenna arrays in fading channels in [11] and [12] for the decorrelator and the optimum joint decoder, respectively. As Gaussian random sequences are subject to random fluctuations of their energies,

Manuscript received June 18, 1998; revised August 24, 1999. The material in this paper was presented in part at the IEEE German Chapter Workshop Kommunikationstechnik, Ulm, Germany, January 1997 and at the 37th Annual Allerton Conference on Communications, Control and Computing, Monticello, IL, Sept. 1999.

The author was with the Telecommunications Laboratory, University of Erlangen-Nuremberg, Erlangen, Germany. He is now with the Vienna Research Center for Telecommunications, Vienna, Austria (e-mail: mueller@ftw.at).

Communicated by U. Madhow, Associate Editor for Detection and Estimation.

Publisher Item Identifier S 0018-9448(01)00463-1.

they lead to a smaller capacity than spherical sequences due to Jensen's inequality.

Multiuser communication systems are described by their capacity region [13] which is given by a set of constraints on the capacities C_i, $1 \le i \le K$, of the individual users transmitting at power level P_i, $1 \le i \le K$. If the total transmission rate is maximum, for the AWGN channel the constraint

$$\sum_{i=1}^{K} C_i = \log_2\left(1+\sum_{i=1}^{K}\frac{P_i}{N}\right)$$

bites [13] with N denoting the noise variance. Assuming that all users want to transmit the same amount of data within the same time and bandwidth, i.e., $C_i = C, \forall i$, we get

$$\frac{2^{KC}-1}{KC} = \frac{1}{K}\sum_{i=1}^{K}\frac{E_{b_i}}{N_0} \triangleq \frac{\overline{E_b}}{N_0} \tag{2}$$

with implicit definitions of the average energy per bit $\overline{E_b}$ and the noise power density N_0.

As CDMA involves an inherent bandwidth expansion by the spreading factor L, spectral efficiency (total capacity per chip) relates to single-user capacity C (capacity per user and symbol) like

$$\Gamma = \frac{K}{L}C \triangleq \zeta C \tag{3}$$

cf. [14], where ζ is termed *load*. In order to illustrate the performance of CDMA in the power-bandwidth plane we need to find a relationship between spectral efficiency Γ and the average energy per bit to noise power density $\overline{E_b}/N_0$.

II. Analysis of Decorrelation

Spectral efficiency of decorrelation with random spreading sequences has been addressed in [15] and [16] by using bounds on the average signal-to-noise (SNR) ratio and Monte Carlo methods. Asymptotic results, i.e., the number of users K and the spreading factor L growing over all bounds, have recently been given in [6] and [7] for binary sequences and, earlier, for spherical sequences in [5]. In this section which is an extended version of [5], we also examine the case of finite K and L.

The probability density function (pdf) of the total distortion (interference and noise) is Gaussian, as the decorrelator completely suppresses all interference. Thus, the main problem to be solved is to derive the statistics of the SNR at the decorrelator output.

The following proposition is proven in Appendix A:

Proposition 1: The probability density function of the SNR after decorrelation in a synchronous CDMA system with K unit-power users, AWGN of variance N, and randomly chosen spherical spreading sequences of length L is given by

$$p_{\gamma_{\rm dec}}(y) = \begin{cases} N\dfrac{(Ny)^{L-K}(1-Ny)^{K-2}}{B(L-K+1,\,K-1)}, & 0 \le y \le 1/N \\ 0, & \text{otherwise} \end{cases} \tag{4}$$

with

$$B(a,\,b) \triangleq \int_0^1 t^{a-1}(1-t)^{b-1}\,dt \tag{5}$$

denoting the beta function.

Note that the pdf of the SNR given by (4) is not only a tool to calculate spectral efficiency; it can also be used to determine the performance variability of decorrelating detectors. Studies on performance variability were previously only available through simulations or approximations [17].

Using (5) the SNR's mth moment can be expressed by

$$\begin{aligned} \underset{\boldsymbol{S}}{E}\{\gamma_{\rm dec}^m\} &= \frac{B(L-K+1+m,\,K-1)}{N^m B(L-K+1,\,K-1)} \\ &= \frac{(L-K+1)_{K-1}}{N^m(L-K+1+m)_{K-1}} \\ &\overset{m\ge 0}{=} \frac{(L-K+1)_m}{N^m(L)_m} \end{aligned} \tag{6}$$

with

$$(x)_m \triangleq \prod_{i=0}^{m-1}(x+i) = \frac{\Gamma(x+m)}{\Gamma(x)} \tag{7}$$

denoting the Pochhammer polynomials, see, e.g., [18, Ch. 18] and $\Gamma(\cdot)$ denoting the gamma function.[1]

The mean[2] of the decorrelator's SNR is given by specializing (6) to

$$\overline{\gamma}_{\rm dec} \triangleq \underset{\boldsymbol{S}}{E}\{\gamma_{\rm dec}\} = \frac{L-K+1}{NL} \tag{8}$$

and the variance by

$$\begin{aligned} \mathrm{Var}\{\gamma_{\rm dec}\} &= \underset{\boldsymbol{S}}{E}\{\gamma_{\rm dec}^2\} - \overline{\gamma}_{\rm dec}^2 \\ &= \frac{(L-K+1)(K-1)}{N^2(L+1)L^2}. \end{aligned} \tag{9}$$

Asymptotically, i.e., $K = \zeta L \to \infty$, $\zeta \in (0;\,1]$, the variance of the SNR vanishes

$$\lim_{K=\zeta L\to\infty} \mathrm{Var}\{\gamma_{\rm dec}\} = 0.$$

The pdf thus degenerates to

$$\lim_{K=\zeta L\to\infty} p_{\gamma_{\rm dec}}(y) = \delta\left(\frac{1-\zeta}{N} - y\right).$$

These properties of the SNR of the decorrelator's output signal are used in the following to give insight into the tradeoff between power and bandwidth efficiency of the decorrelator.

Let the capacity averaged over all sets of spherical sequences be denoted by

$$\overline{C}_{\rm dec} \triangleq \underset{\boldsymbol{S}}{E}\{C_{\rm dec}\} = \underset{\boldsymbol{S}}{E}\{\log_2(1+\gamma_{\rm dec})\}.$$

In Appendix B, the following proposition is proven.

Proposition 2: The average channel capacity of a unit power CDMA channel which is disturbed by complex AWGN of vari-

[1]Note that $\Gamma(\cdot)$ denotes the gamma function while Γ denotes spectral efficiency.

[2]The first moment (mean) has already been found in [2] searching for a lower bound on the mean SNR of the minimum mean-squared error (MMSE) detector.

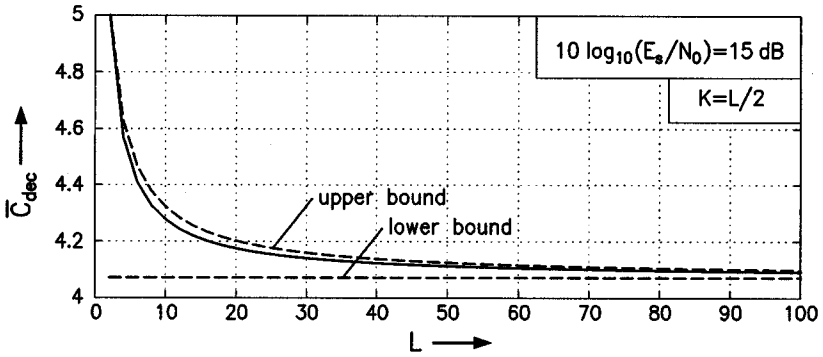

Fig. 1. Average channel capacity $\overline{C}_{\rm dec}$ with the decorrelation versus spreading factor L for $K = L/2$ and $10\log_{10}(E_s/N_0) = 15$ dB. The dashed lines refer to the upper and lower bound, respectively.

ance N with K users which are separated by decorrelation is given by

$$\overline{C}_{\rm dec} = \log_2\left(1+\frac{1}{N}\right) - \log_2(e)\sum_{i=1}^{\infty}\frac{(K-1)_i}{n(L)_i}\left(\frac{1}{1+N}\right)^i \tag{10}$$

and bounded by

$$\log_2\left(1+\frac{L-K}{NL}\right) < \overline{C}_{\rm dec} < \log_2\left(1+\frac{L-K+1}{NL}\right) \tag{11}$$

if the spreading sequences are uniformly distributed on the $(L-1)$-dimensional surface of an L-sphere.

Proposition 2 implies some surprising consequences. Channel capacity is a concave function of the random SNR. Thus, the average capacity is lower than capacity at the average SNR, see (8), which gives the right-hand side of (11). It is obvious from (9) that the variance of the SNR is a decreasing function of L and vanishes for infinite spreading factor. This should imply that capacity reaches its maximum for infinite L if the load $\zeta = K/L$ is fixed. Surprisingly, this statement is disproved by the left-hand side of (11). In fact, the average SNR depends on the *interference* load $(K-1)/L$ and for fixed interference load $(K-1)/L$ the above statement actually holds. Since users do not interfere with themselves, the interference load is smaller than the user load. This effect is beneficial for small spreading gains L and vanishes asymptotically; it overrules the impact of decreasing variance of SNR. This means that the *asymptotic capacity in terms of the load $\zeta = K/L$ is a lower bound on the nonasymptotic capacity*. Therefore, it is referred to as the main figure of merit for comparison with other multiuser detectors in Section V. As depicted in Fig. 1, the upper bound is much tighter than the lower bound.

Using (3) and Proposition 2, the asymptotic relationship between power and bandwidth efficiency results in

$$\lim_{K=\zeta L\to\infty}\left(\frac{E_b}{N_0}\right)_{\rm dec} = \frac{2^{\Gamma_{\rm dec}/\zeta}-1}{\Gamma_{\rm dec}/\zeta - \Gamma_{\rm dec}} \tag{12}$$

and is illustrated in Fig. 2. It was reported in [5] for the first time. Subsequently, Verdú and Shamai [6], [7] found the same result for binary sequences. As will be seen in Section V, this holds for a much wider class of random sequence models. Fig. 2 indicates that the parameter ζ has to be carefully adjusted for high spectral efficiency. For the decorrelator, no closed-form solution for the optimum load has yet been found. Thus, a numerical optimization has been used resulting in the solid line in Fig. 6 (Section IV).

Fig. 2 shows a large gap between the orthogonal system and one applying CDMA with random sequences and decorrelation. However, Fig. 2 does not indicate whether this gap remains constant for large spectral efficiencies or continues to increase. This is investigated in the following.

Applying (11), the performance loss of the decorrelator in terms of power efficiency compared to the single-user Shannon bound is given by

$$V_{\rm dec}(\Gamma) \triangleq \frac{\min\limits_{\zeta}\left(\frac{E_b}{N_0}\right)_{\rm dec}}{\frac{2^\Gamma-1}{\Gamma}} = \min_{\zeta}\frac{2^{(1/\zeta-1)\Gamma}-2^{-\Gamma}}{(1-2^{-\Gamma})(1/\zeta-1)}.$$

By Taylor expansion, we get

$$V_{\rm dec}(\Gamma) = \min_{\zeta}\frac{2^{(1/\zeta-1)\Gamma}}{1/\zeta-1} + \frac{\mathcal{O}\left(2^{(1/\zeta-2)\Gamma}\right)}{1/\zeta-1}. \tag{13}$$

The simple optimization problem in (13) can be solved by first-order derivation. Its solution reads

$$\zeta_{\rm opt} \longrightarrow \frac{1}{1+\dfrac{\log_2 e}{\Gamma}}$$

yielding

$$V_{\rm dec}(\Gamma) = \frac{e}{\log_2 e}\,\Gamma + \mathcal{O}(\Gamma 2^{-\Gamma}). \tag{14}$$

Thus, the asymptotic loss, i.e., $V_{\rm dec}(\Gamma)$, $\Gamma\to\infty$, is proportional to spectral efficiency. For spectral efficiency larger than $\Gamma \approx 4$, the difference from the exact loss is very small. The loss when compared to the interference-free case grows over all bounds if spectral efficiency does. Nevertheless, this is an important improvement in comparison to the conventional detector, whose loss becomes infinite for a *finite* spectral efficiency because of interference limitation.

III. Conventional Matched-Filtering

Spectral efficiency of conventional CDMA has been extensively studied in the literature [19]–[23], [14], [24], [3],

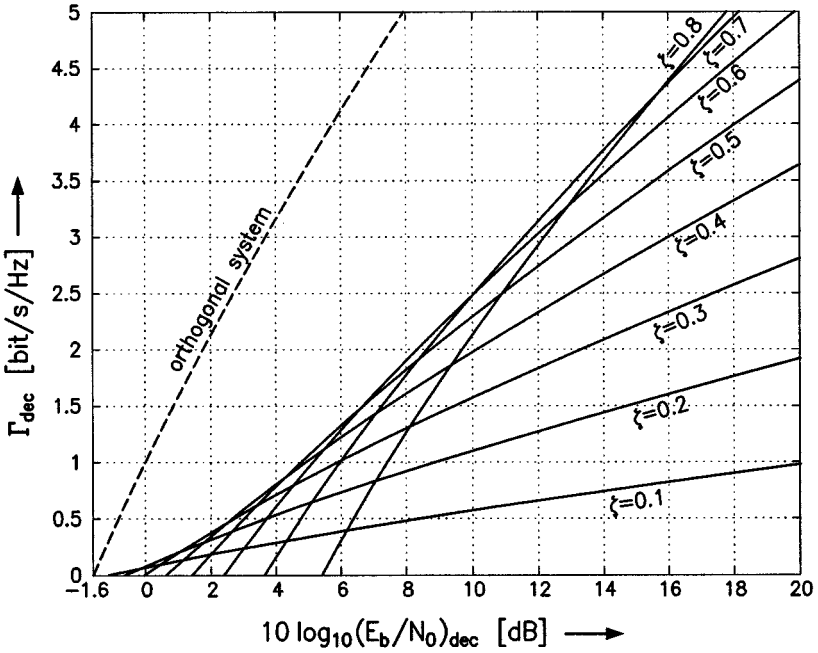

Fig. 2. Power-bandwidth-plane for the decorrelator with load ζ as parameter. For comparison the dashed line shows an orthogonal system.

[6], [4], [7]. However, these references are either asymptotic in the number of users, or based on approximations and/or Monte Carlo simulations. Here, spectral efficiency for spherical random sequences of finite length is calculated analytically.

In the following, each interfering signal is modeled as white Gaussian noise which is the worst case additive noise for power-constrained inputs. Note that for discrete alphabets non-Gaussian noise may be worse [25]. For the purpose of maximum mutual information, the coded symbols are also assumed to follow a Gaussian distribution. Based on these assumptions, the information rate of user k becomes

$$C_{\mathrm{con},\,k} = \log_2(1+\gamma_{\mathrm{con},\,k})$$

with the SINR of user k given by [26]

$$\gamma_{\mathrm{con},\,k} = \frac{1}{N + \sum\limits_{i\neq k} (\boldsymbol{S}^H\boldsymbol{S})_{ki}^2}.$$

Proposition 3: The average capacity of the unit power K-user CDMA channel with spherical random sequences of length L, which is disturbed by complex AWGN of variance N, is given by

$$\overline{C}_{\mathrm{con}} = (L-1)!^{(K-1)}\log_2(e) \cdot \int_0^\infty \Re\left\{\gamma^*(L-1,\,-j\omega)^{K-1} e^{-j\omega(K+N)}(e^{j\omega}-1)\right\}\frac{d\omega}{\omega} \quad (15)$$

and bounded by

$$\overline{C}_{\mathrm{con}} > \log_2\left(1+\frac{1}{N+\frac{K-1}{L}}\right) \quad (16)$$

with

$$\gamma^*(a,\,x) \triangleq \int_0^1 e^{-xt}t^{a-1}\,dt/(a-1)!$$

denoting the entire incomplete gamma function.

The proof is placed in Appendix C. Comparing the bounds in Propositions 2 and 3, an essential difference becomes obvious. The bound obtained from Jensen's inequality is an upper bound for the decorrelator and a lower bound for conventional demodulation, see (11) and (16), respectively. This is, as for decorrelation, the SINR is averaged, while for conventional detection the mean of interference power which is the reciprocal of SINR is used in the considerations. Fig. 3 compares the lower bound to the exact average capacity and illustrates a significant gap for short sequences.

IV. Decorrelating Decision Feedback

Combining decorrelating decision-feedback with channel coding, there are a few different realizations one can think about. The one considered here is depicted in Fig. 4 for the two-user case. The cancellation of interfering signals is performed after the decoding process. This provides (almost) error-free feedback.

In contrast to linear decorrelation, decorrelating decision-feedback is asymmetric in the user direction. That is, the users do not operate under the same conditions. Some users are more and some are less disturbed by multiuser interference *on average*. This fact has significant impact on cellular communications design [27]–[30]. It implies that the signals of users transmitting at identical SNRs may be characterized by different SINRs after multiuser detection and *average* channel capacities differ among the users. As a corollary, we can state that users with equal average channel capacities require different SNRs. Although there exist many cases with different joint rate *and* SNR distributions among the users, we distinguish only the two cases previously mentioned in this paragraph, i.e., the equal rate and the equal power cases.

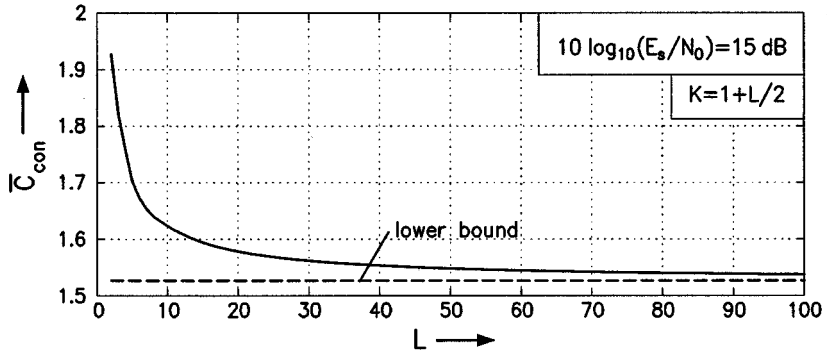

Fig. 3. Average channel capacity $\overline{C}_{\text{con}}$ for the conventional matched-filter receiver and spherical random spreading by a factor of L for $K = 1 + L/2$ and $10 \log_{10}(E_s/N_0) = 15$ dB. The dashed line refers to the lower bound.

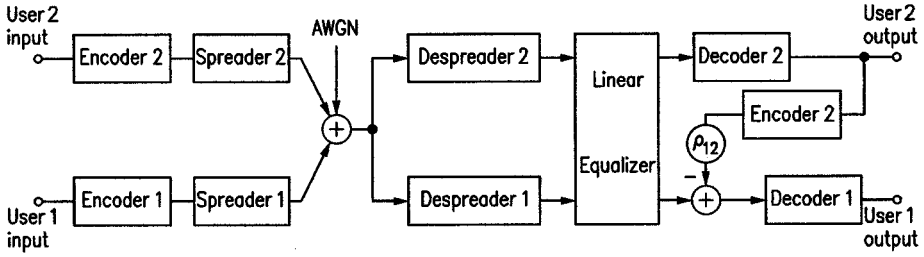

Fig. 4. Structure of decision-feedback decoding for two users.

A. Equal Powers

In the following, we assume that all users are received with identical SNR, i.e., their ratio of energy per symbol to noise power density is fixed. This enables us to obtain the average capacity of decorrelating decision feedback by averaging the average capacity of the decorrelating detector with k users given by (10), see Proposition 2, over a discrete uniform distribution of users $1 \le k \le K$. In Appendix D, we prove the following proposition.

Proposition 4: The average channel capacity of a CDMA channel with K users of unit powers which is disturbed by complex AWGN of variance N and includes a decorrelating decision-feedback receiver is given by

$$\overline{C}_{\text{decDF1}} = \log_2\left(1+\frac{1}{N}\right) - \log_2(e)\,\frac{K-1}{K}\sum_{i=1}^{\infty}\frac{(K)_i}{i(i+1)(L)_i}\left(\frac{1}{1+N}\right)^i \quad (17)$$

and is bounded by

$$\frac{K-1}{K}\,f\left(\frac{K+1}{L(1+N)}\right) < \overline{C}_{\text{decDF1}} - \log_2\left(1+\frac{1}{N}\right) < \frac{K-1}{K}\,f\left(\frac{K}{L(1+N)}\right)$$

with

$$f(x) \triangleq \left(1-\frac{1}{x}\right)\log_2(1-x) - \log_2 e$$

if the spreading sequences are uniformly distributed on the $(L-1)$-dimensional surface of an L-sphere.

Unfortunately, (17) does not illustrate the influence of the parameters K, L, N denoting number of users, spreading factor, and noise variance, respectively. For this purpose, it is more helpful to examine the asymptotic behavior, i.e., as the number of users grows over all bounds but the load remains constant. Asymptotically, both bounds given in Proposition 4 coincide yielding

$$\lim_{K=\zeta L\to\infty}\overline{C}_{\text{decDF1}} = \log_2\left(1+\frac{1-\zeta}{N}\right) - \frac{1+N}{\zeta}\log_2\left(1-\frac{\zeta}{1+N}\right) - \log_2 e.$$

It follows from (17) that the asymptotic average capacity is a strictly decreasing function of the number of users K. For the decorrelator, the number of users is upper-bounded by the spreading factor [10]. This means that the minimal asymptotic average capacity is achieved for $K = L$ and is given by

$$\min_{\zeta\le 1}\lim_{K=\zeta L\to\infty}\overline{C}_{\text{decDF1}} = (1+N)\log_2\left(1+\frac{1}{N}\right) - \log_2 e.$$

Surprisingly, the asymptotic loss in capacity, i.e., the gap between orthogonal sequences and randomly chosen ones, is less than *1 nat* (about 1.44 bits)

$$\min_{\zeta<1}\lim_{K=\zeta L\to\infty}\log_2\left(1+\frac{1}{N}\right) - \overline{C}_{\text{decDF1}} = \log_2(e) - N\log_2\left(1+\frac{1}{N}\right). \quad (18)$$

It vanishes for $N \to \infty$ and achieves the maximal value of 1 nat for $N \to 0$.

Comparing this with the results found for the optimum joint demodulator, see [6], [7], we find that the decorrelating decision-feedback receiver is asymptotically optimal if the number

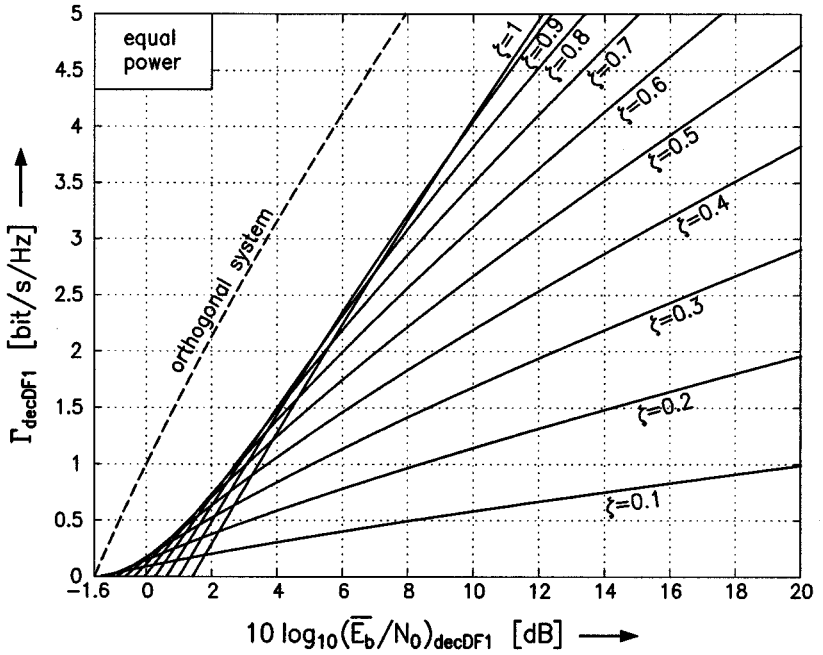

Fig. 5. Power-bandwidth-plane for the decorrelating decision-feedback receiver with load ζ as parameter and equal powers for all users. For comparison the dashed line shows an orthogonal system.

of users equals the spreading factor and the powers of the users are identical, but their rates differ. This can also be generalized to all loads implied by a more general result, see Proposition 5 (Section V). Moreover, it is the counterpart in multiuser detection to a result found by Price [31], [32] for equalization of intersymbol interference (ISI) where zero-forcing decision-feedback equalization is also asymptotically optimum, as $N \to 0$.

When considering spectral efficiency instead of average capacity, a low number of users is not optimal, cf. Section II. Fig. 5 shows, that in this case the optimal load depends on SNR. Note also that the loss in spectral efficiency is larger than 1 nat for unit load. This is, as spectral efficiency is plotted versus the energy per *bit* which depends on the average capacity. In contrast, (18) is based on the energy per symbol. Nevertheless, (18) can be used to calculate the asymptotic loss in power efficiency. As the optimum load converges to 1 for large spectral efficiencies, cf. Fig. 6, the asymptotic power loss is bounded by

$$V_{\mathrm{decDF1}}(\Gamma) = \frac{\min\limits_{\zeta}\left(\frac{\overline{E_b}}{N_0}\right)_{\mathrm{decDF1}}}{\frac{2^{\Gamma}-1}{\Gamma}} < \frac{\frac{2^{\Gamma+\log_2 e}-1}{\Gamma+\log_2 e}}{\frac{2^{\Gamma}-1}{\Gamma}} = e + \mathcal{O}(\Gamma^{-1}). \tag{19}$$

As (19) shows, the loss of only 1 nat in spectral efficiency—which obviously corresponds to a factor e in power efficiency—is achieved at least asymptotically for $\frac{E_b}{N_0} \to \infty$.

B. Equal Rates

In contrast to the equal power case discussed in the previous section, the pre-assumption of equal rates prohibits an explicit expression giving the average capacity, as the problem of optimal power assignment cannot be solved analytically for finite spreading gain. Nevertheless, the average capacity can be bounded for all users with the help of Proposition 2

$$\log_2\left(1+\frac{L-k}{L}\cdot\frac{E_k}{N_0}\right) < \overline{C}_{\mathrm{decDF2}} < \log_2\left(1+\frac{L-k+1}{L}\cdot\frac{E_k}{N_0}\right)$$

with E_k denoting the energy per symbol of user k. These bounds yield for the users' individual SNRs

$$\frac{2^{\overline{C}_{\mathrm{decDF2}}}-1}{1-(k-1)/L} < \frac{E_k}{N_0} < \frac{2^{\overline{C}_{\mathrm{decDF2}}}-1}{1-k/L}.$$

The energies per symbol and per bit averaged over all users are then bounded by

$$\sum_{k=1}^{K}\frac{1}{L-k+1} < \frac{\frac{K}{L}\cdot\frac{\overline{E_s}}{N_0}}{2^{\overline{C}_{\mathrm{decDF2}}}-1} < \sum_{k=1}^{K}\frac{1}{L-k}$$

$$\int_0^K \frac{dy}{L-y+1} < \frac{\frac{K}{L}\cdot\frac{\overline{E_s}}{N_0}}{2^{\overline{C}_{\mathrm{decDF2}}}-1} < \int_1^{K+1}\frac{dy}{L-y}$$

$$\ln\frac{L+1}{L-K+1} < \frac{\frac{K}{L}\cdot\frac{\overline{E_s}}{N_0}}{2^{\overline{C}_{\mathrm{decDF2}}}-1} < \ln\frac{L-1}{L-K-1}$$

and

$$\ln\frac{L+1}{L-K+1} < \frac{\Gamma_{\mathrm{decDF2}}\left(\frac{\overline{E_b}}{N_0}\right)_{\mathrm{decDF2}}}{2^{\Gamma_{\mathrm{decDF2}}L/K}-1} < \ln\frac{L-1}{L-K-1}$$

respectively. In the asymptotic case both bounds coincide. Thus, we have[3]

$$\lim_{K=\zeta L\to\infty}\left(\frac{\overline{E_b}}{N_0}\right)_{\mathrm{decDF2}} = -\ln(1-\zeta)\,\frac{2^{\Gamma_{\mathrm{decDF2}}/\zeta}-1}{\Gamma_{\mathrm{decDF2}}}. \tag{20}$$

This relationship is illustrated for several values of the load ζ in Fig. 7. Looking at large SNRs, the gap to the orthogonal bound is

[3]This formula could also be gained from the results found independently in [10, pp. 376–377] where error-free feedback is assumed implicitly via $N \to 0$.

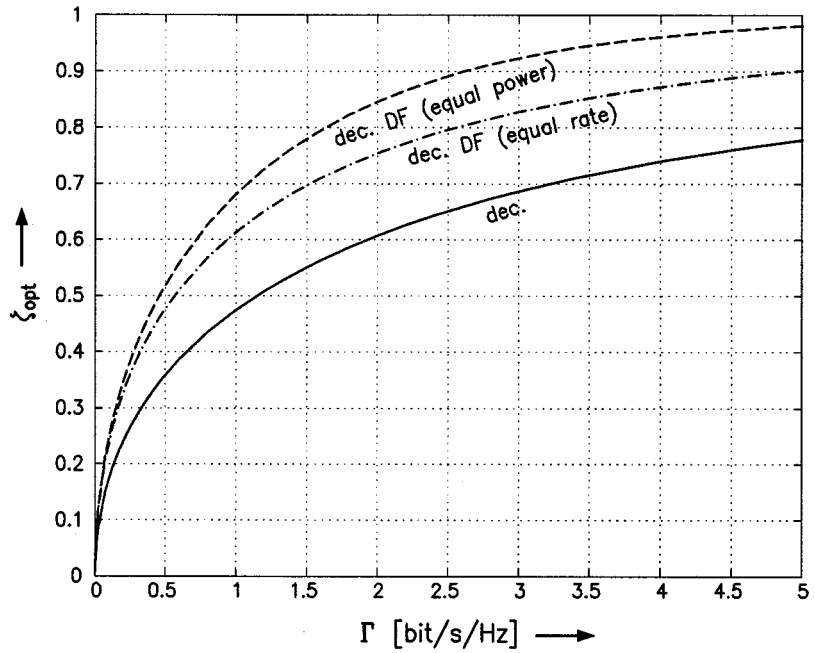

Fig. 6. Ratios of users to spreading factor ζ_{opt} that maximize spectral efficiency Γ_{dec} (solid line), Γ_{decDF1} (dashed line), and Γ_{decDF2} (dash-dotted line), respectively.

smaller than without decision feedback, but slightly larger than in the equal-power case. The asymptotic loss is bounded by

$$V_{\mathrm{decDF2}}(\Gamma) = \frac{\min\limits_{\zeta}\left(\frac{E_b}{N_0}\right)_{\mathrm{decDF2}}}{\frac{2^{\Gamma}-1}{\Gamma}} = \frac{\inf\limits_{c}\lim\limits_{\zeta\to\frac{\Gamma}{\Gamma+c}}\left(\frac{E_b}{N_0}\right)_{\mathrm{decDF2}}}{\frac{2^{\Gamma}-1}{\Gamma}}$$

for some positive constant c. With (20), the asymptotic loss can be shown by Taylor expansions to be

$$V_{\mathrm{decDF2}}(\Gamma) = \min_{c>0} 2^c \ln\left(1+\frac{\Gamma}{c}\right)\left(1+\mathcal{O}(2^{-\Gamma})\right). \quad (21)$$

The asymptotic loss of the decorrelator is proportional to spectral efficiency, see (14), while it is constant for decorrelating decision feedback with equal powers, cf. (19). For equal rates, it is shown in (21) to be proportional to the logarithm of spectral efficiency. This is a significant improvement compared to decorrelation without decision feedback and only a small degradation from the performance in the equal power case.

V. Comparison and Conclusion

In this section, we give a comparison of the previously obtained results for the decorrelating and decorrelating decision-feedback detector with the ones found by other authors, e.g., [6], [7] for different detection schemes.

Although the results in these references are mostly restricted to binary random spreading, they extend to a much wider class of random sequence sets. As shown by recent results in random matrix theory [33], the asymptotic eigenvalue distributions of random covariance matrices are independent of the particular distributions of random chips under mild conditions. Sufficient, but not necessary conditions of this are the existence of the fourth moment of the chips' pdf [34] and the mutual independence of the chips. For spherical random sequences, the latter conditions are at least fulfilled asymptotically. In conjunction with the asymptotic convergence properties of the SINR of several linear multiuser receivers reported in [8] and [9], this justifies the application of asymptotic results on spectral efficiency which were originally found for binary random sequences to spherical random sequences, as well.

A. Results for Other Detectors

Asymptotic spectral efficiency of conventional demodulation has extensively been studied in the literature [21]–[23], [14], [6], [7]. The final result reads

$$\lim_{K=\zeta L\to\infty} \overline{C}_{\mathrm{con}} = \log_2\left(1+\frac{1}{N+\zeta}\right). \quad (22)$$

Spectral efficiency $\Gamma = \zeta\overline{C}$ is strictly increasing with the load. With the same procedure as used in Section IV-B, i.e., resolving (22) to the SNR and averaging over the load, we get the power efficiency of the conventional decision-feedback receiver with equal rates, cf. [28, eq. 12]

$$\lim_{K=\zeta L\to\infty}\left(\frac{\overline{E_b}}{N_0}\right)_{\mathrm{conDF2}} = \frac{\exp\left(\zeta(2^{\Gamma/\zeta}-1)\right)-1}{\Gamma}. \quad (23)$$

Considering conventional decision feedback with equal powers we get the average capacity by averaging (22) with respect to ζ

$$\lim_{K=\zeta L\to\infty}\overline{C}_{\mathrm{conDF1}} = \frac{1}{\zeta}\int_0^{\zeta}\lim_{K=\zeta' L\to\infty}\overline{C}_{\mathrm{con}}\,d\zeta' = \frac{1}{\zeta}\int_0^{\zeta}\log_2\left(1+\frac{1}{N+\zeta'}\right)d\zeta'.$$

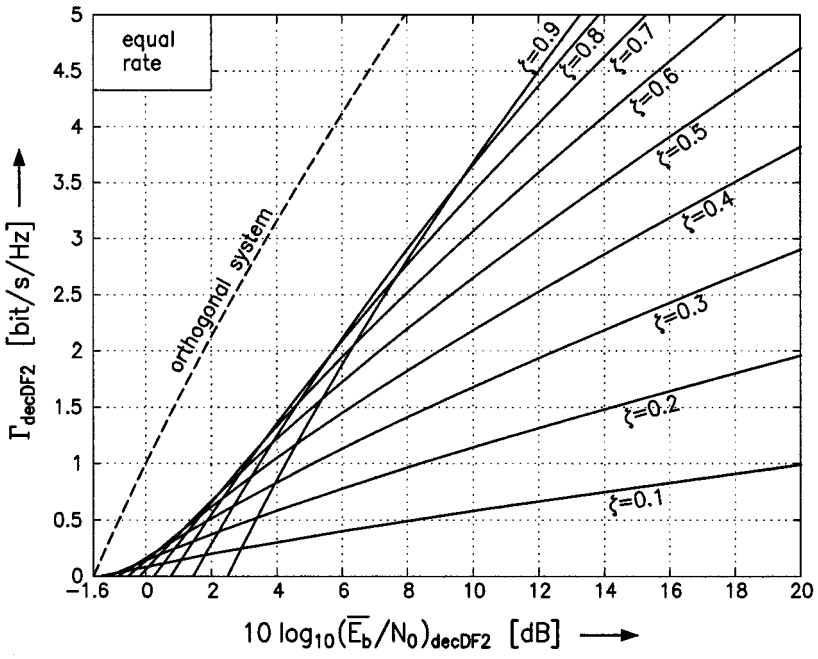

Fig. 7. Power-bandwidth-plane for the decorrelating decision-feedback receiver with load ζ as parameter and equal rates for all users. For comparison the dashed line shows an orthogonal system.

With change of variables ($y \triangleq 1 + 1/(N+\zeta)$) and [35, eq. 2.727.3] we finally obtain

$$\lim_{K=\zeta L\to\infty} \overline{C}_{\text{conDF1}} = \frac{1}{\zeta}\left((\zeta+N)\log_2\left(1+\frac{1}{N+\zeta}\right) - N\log_2\left(1+\frac{1}{N}\right) + \log_2\left(1+\frac{\zeta}{1+N}\right)\right).$$

Spectral efficiency of the MMSE detector has been examined with the help of Monte Carlo methods in [36]. The later analytical result

$$\lim_{K=\zeta L\to\infty} \overline{C}_{\text{mmse}} = \log_2\left(1+\frac{1}{N}-\frac{1}{4}\left(\sqrt{1+\frac{\left(1+\sqrt{\zeta}\right)^2}{N}} - \sqrt{1+\frac{\left(1-\sqrt{\zeta}\right)^2}{N}}\right)^2\right) \quad (24)$$

is due to [6] and [7].

The result for the optimal joint demodulator

$$\lim_{K=\zeta L\to\infty} \overline{C}_{\text{Opt}} = \frac{1}{2\pi\zeta}\int_{(1-\sqrt{\zeta})^2}^{(1+\sqrt{\zeta})^2} \log_2\left(1+\frac{y}{N}\right) \cdot \sqrt{\left(y-\left(1-\sqrt{\zeta}\right)^2\right)\left(\left(1+\sqrt{\zeta}\right)^2-y\right)}\,\frac{dy}{y} \quad (25)$$

is reported in [6].[4]

[4]An alternative representation of (25) that does not contain an integration, but is also lengthy, can be found in [7].

With the help of (3) it is straightforward to obtain spectral efficiency from (22), (24), and (25). For MMSE decision feedback, the following proposition holds.

Proposition 5: For any given number of users and any given set of spreading sequences, the total capacity of a system applying the MMSE decision-feedback receiver and single-user channel coding equals the capacity of a system with optimal joint multiuser decoding.

This proposition follows straightforwardly from [37]. Proposition 5 is the counterpart in multiuser theory to the known optimality of MMSE decision-feedback equalization for ISI channels shown in [38] and [39]. Unlike in the ISI case, where the assumption of error-free feedback incurs serious problems [40] due to causality reasons, on the synchronous Gaussian multiple-access channel (GMAC) error-free decision feedback can be provided by re-encoding of the previous users.

The average capacity of the MMSE decision-feedback receiver with equal powers and the average capacity of optimal joint demodulation equal each other due to Proposition 5, i.e.,

$$\overline{C}_{\text{mmseDF1}} = \overline{C}_{\text{Opt}}.$$

As already found in Section IV, equal power design is preferable for decorrelating decision feedback, when compared to equal-rate design. This even holds for large SNRs, where decorrelation becomes asymptotically equivalent to MMSE-based receiver design. Therefore, the question arises, why this is not a contradiction to Proposition 5 stating the optimality of MMSE decision feedback. Which restrictions needed for Proposition 5 are violated by the equal-rate assumption and thus prohibit its application in this case? Note that Proposition 5 only states the optimality of MMSE decision feedback for given powers (implicitly given by the demand for a given set a sequences). Moreover, the maximization of total capacity for

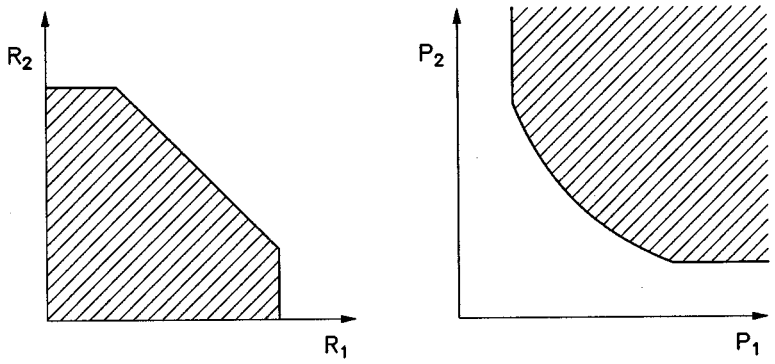

Fig. 8. Capacity and power regions for two users and $|\rho_{12}|^2 = 0.85$.

given powers E_k, $1 \le k \le K$, and minimization of total power for given information rates R_k, $1 \le k \le K$, are different aims on a general correlated waveform Gaussian multiple-access channel. This is illustrated in Fig. 8 for the two-user case with the correlation coefficient ρ_{12} by showing the achievable rate region and the required power region on the left- and right-hand side, respectively. The vertices of the capacity region achieve total capacity, while the vertices of the power region do not achieve the minimal total power, in general. This can also be seen by the mathematical formulation of the problem [41]

$$\begin{aligned} R_1 &\le \log_2\left(1+\frac{P_1}{N}\right) \\ R_2 &\le \log_2\left(1+\frac{P_2}{N}\right) \\ R_1+R_2 &\le \log_2\left(1+\frac{P_1+P_2}{N}+(1-|\rho_{12}|^2)\,\frac{P_1P_2}{N^2}\right). \end{aligned}$$

While the information rates are only combined by linear equations, solving for equivalent explicit conditions on the powers leads to nonlinear combinations of the information rates if $0 \neq |\rho_{12}| \neq 1$.

The previous paragraph suggests a degradation of MMSE decision feedback in the equal-rates case. However, this loss does not need to be significant. A quantitative analysis of MMSE decision feedback with equal rates is given in the following:

Let $\gamma_{\mathrm{mmse},k}$ denote the SINR of the kth user after a linear MMSE front and *without decision feedback* and the number of users grows over all bounds. Then, as shown by Tse and Hanly [8], [9], the users' powers and SINRs are interconnected by

$$\frac{P_k}{\gamma_{\mathrm{mmse},k}} = N + \lim_{K\to\infty}\frac{\zeta}{K}\sum_{\substack{i=1\\ i\neq k}}^{K}\frac{P_kP_i}{P_k+P_i\gamma_{\mathrm{mmse},k}} \qquad \forall\, k.$$

In order to get a corresponding equation for the MMSE decision-feedback receiver, we make use of the fact that all previously demodulated users do not interfere with the instantaneously demodulated user. This can easily be taken into account by setting the power of the previously demodulated users to zero. Demodulating the users in descending order of their indexes, cf. Fig. 4, implies that the powers of all users with indexes greater than the instantaneous one vanish.

If all users' rates are equal, the users' SINRs are equal too, since single-user coding is used. Thus, with $\gamma_{\mathrm{mmseDF2}}$ denoting the SINR of the MMSE decision-feedback receiver with equal rates, we have

$$\frac{P_k}{\gamma_{\mathrm{mmseDF2}}} = N + \lim_{K\to\infty}\frac{\zeta}{K}\sum_{i=1}^{k-1}\frac{P_kP_i}{P_k+P_i\gamma_{\mathrm{mmseDF2}}} \qquad \forall\, k.$$

Although this does not lead to an analytical expression for the required sum power given a certain SINR, it enables recursive numerical computation of the users' powers.

B. Comparison of the Results

In Fig. 9, the several (sub)optimal receivers are compared by their spectral efficiencies in the power-bandwidth plane. First, it illustrates the interference limitation of the conventional receiver. Second, it shows the asymptotic equivalence of the MMSE receiver with the conventional matched filter and the decorrelator for low and high SNRs, respectively. Third, the asymptotic convergence of the decorrelating decision-feedback receiver to the MMSE decision-feedback receiver is illustrated for both the equal- rate and the equal-power cases. Moreover, the performance gap between the equal-rate and the equal-power case is small.

Proposition 5 showed that the MMSE decision-feedback receiver with equal powers is overall optimum. For providing equal rates only a little more power is required if decision-feedback receivers are employed. This small gap can be closed using optimum joint coding or time sharing between virtual rate tuples that are vertices of the corresponding capacity region. However, a gap in spectral efficiency remains when compared to an orthogonal system. This is caused by the eigenvalue spread of the spreading sequences' correlation matrix.

Previously we distinguished the cases of equal power and equal rate for all users. As shown in Fig. 9, the equal-power design is preferable for the decorrelating decision-feedback receiver while the conventional decision-feedback receiver performs better with equal-rate design. This can be understood considering the influence of interfering users' powers onto the multiuser receivers' performances. The decorrelator is not affected by the interfering users' powers, but the conventional receiver suffers heavily from the near–far problem [10]. The demand for equal rates implies the users' powers to be widely spread. As the high-power users are demodulated and canceled first, the interference power is diminished fast. This is advantageous for the conventional detector, but has no impact on the decorrelator.

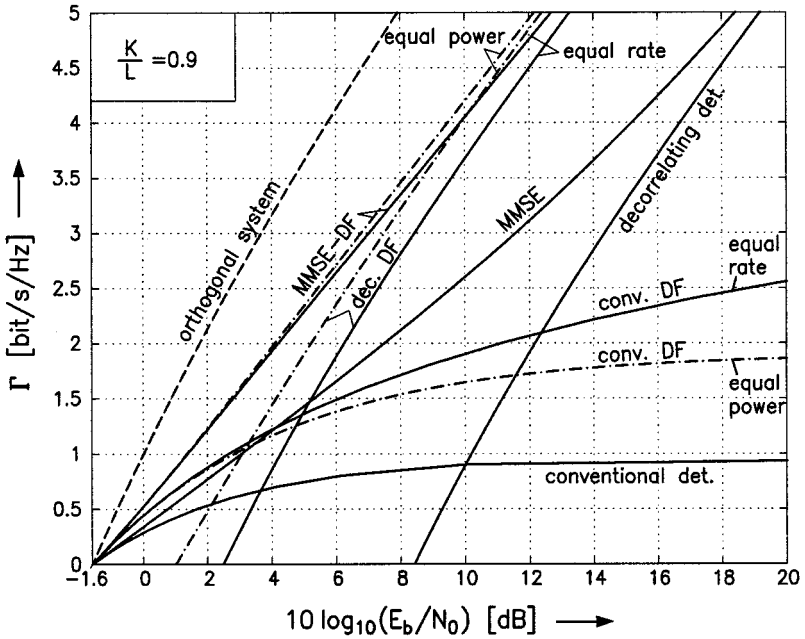

Fig. 9. Power-bandwidth-plane for conventional, decorrelating, and MMSE multiuser receivers with and without decision feedback for load $\zeta = 0.9$. For comparison, the dashed line shows an orthogonal system.

The decorrelator works very well for moderate load, but fails if the number of users approaches the spreading factor. Demand for equal power implies poor performance for the early demodulated users and thus results in a small rate for those users. However, the overall impact on the average rate is small. On the other hand, considering the equal-rate case, we see that many users can deal with low power, but the early demodulated ones require high power and dominate the average power consumption.

Fig. 9 gives the spectral efficiencies for a fixed load which is not the optimum one, i.e., it does not maximize spectral efficiency, in general. In Fig. 10, the corresponding results are shown for optimized loads. As one can observe, there are some similarities, e.g., the behavior of the linear multiuser receivers in the high-SNR range. There are at the same time some fundamental differences: the decorrelating decision-feedback receiver and its MMSE counterpart do not converge to each other. In contrast, the MMSE decision-feedback receivers reach the performance of an orthogonal system. This is understood by the following considerations. It was shown by Viterbi [23] that decision feedback in conjunction with (even) conventional demodulation achieves spectral efficiency of orthogonal systems if the load grows over all bounds. This occurs because in this case the eigenvalue spread of the correlation matrix vanishes [4]. Since the MMSE decision-feedback receiver performs at least as well as the conventional decision-feedback receiver, we expect the same for the MMSE decision-feedback receiver, as well. In contrast, the performance of decorrelating decision feedback is limited as the load cannot exceed 1.

More insight into this topic is obtained from Fig. 11. There, the spectral efficiencies of the various multiuser receivers are depicted versus power efficiency as in Fig. 9, but the load is $\zeta = 2$. MMSE decision feedback approaches the orthogonal bound more closely than it does for a smaller load, cf. Fig. 9. But the linear MMSE receiver yields a much worse performance. It even suffers from interference limitation. Fig. 11 also shows the advantages of MMSE decision feedback over conventional decision feedback . Although both methods are equivalent for $\zeta \to \infty$, MMSE decision feedback converges much faster to the performance bound set by orthogonal systems.

C. Summary and Conclusion

A likely fair basis for comparison of multiuser receivers in (perfectly) coded communication systems has been given. The most common multiuser detectors providing soft information for the channel decoder have been analyzed. The well-known advantages of MMSE detection when compared to conventional and decorrelating detection have been confirmed. The performance variability of the decorrelating detector has been derived analytically and the average capacity has been given for finite number of users. Moreover, the spectral efficiency has been shown to decrease slightly with the spreading factor, if the system load is fixed. Thus, it is *not* necessary to provide large spreading factors in order to neglect the degradation caused by performance variability.

The advantages of linear preprocessing for decision-feedback multiuser receivers have been highlighted, i.e., MMSE decision feedback was deduced to be able to achieve the optimal joint decoders capacity and to be strongly preferable to conventional decision feedback if the load is restricted to values that can be handled in practice. Decorrelating decision-feedback detectors have been found to achieve higher capacity when they are operated with equal-power users rather than with equal-rate users. This suggests the application of a time-sharing or rate-splitting [42] protocol to exploit all theoretical resources. How this can be done in such a way that no loss to the equal-power case occurs has recently been shown in [43].

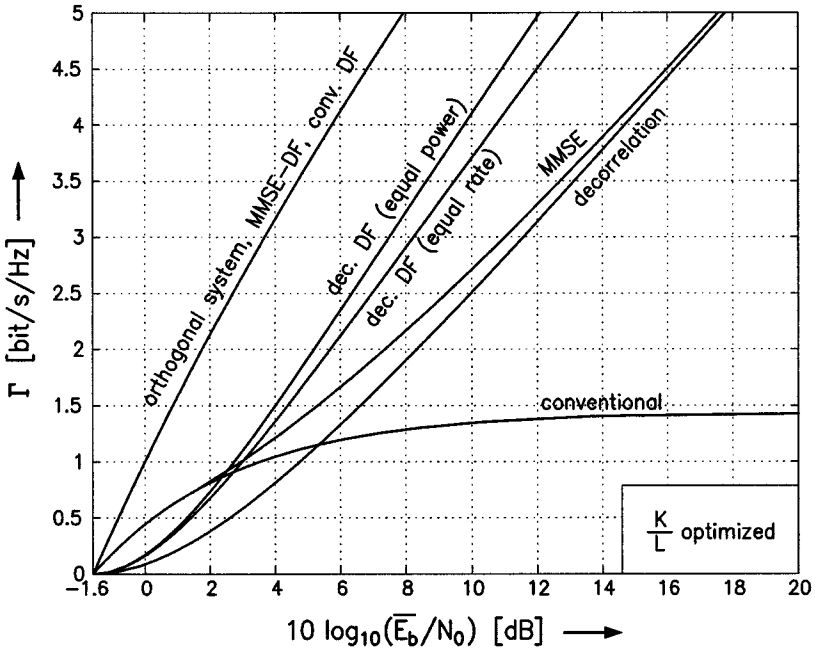

Fig. 10. Power-bandwidth-plane for conventional, decorrelating, and MMSE multiuser receivers with and without decision feedback and optimized load.

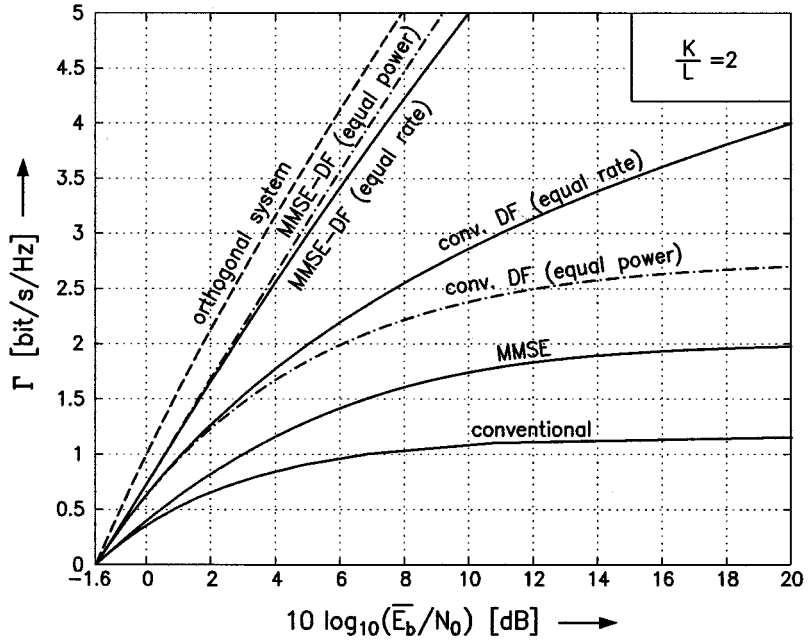

Fig. 11. Power-bandwidth-plane for conventional and MMSE multiuser receivers with and without decision feedback and load $\zeta = 2$. For comparison, the dashed line shows an orthogonal system.

APPENDIX A
PROOF OF PROPOSITION 1

In order to prove the result for the decorrelator's SINR previous results on the SINR of the MMSE receiver are helpful. In [44], the SINR of user k after an MMSE front end for known signature sequences was shown to be

$$\gamma_{\mathrm{mmse},\,k} = \boldsymbol{s}_k^{\mathrm{H}} \boldsymbol{P}^{-1} \boldsymbol{s}_k.$$

Here, $\boldsymbol{P} \triangleq \boldsymbol{S}\boldsymbol{S}^{\mathrm{H}} - \boldsymbol{s}_k \boldsymbol{s}_k^{\mathrm{H}} + N\mathbf{I}$ denotes the covariance matrix of total distortion (interference and noise). The covariance matrix of the total distortion is Hermitian and can be transformed by a unitary transformation into a diagonal matrix. As a unitary transformation does not affect the pdf of spherically distributed random vectors [45, Appendix A.1], the covariance matrix is assumed to be diagonal and its eigenvalues to be λ_i, $1 \le i \le L$ without loss of generality. This implies

$$\gamma_{\mathrm{mmse},\,k} = \sum_{i=1}^{L} \frac{|s_{i,k}|^2}{\lambda_i}$$

and (1) yields

$$\gamma_{\mathrm{mmse},\,k} = \sum_{i=1}^{L} \frac{|g_i|^2}{\lambda_i} \Bigg/ \sum_{i=1}^{L} |g_i|^2. \tag{26}$$

In the case of decorrelation, the power of the interfering users has no effect. Therefore, it can be assumed to be infinite without loss of generality. In this case, the above given equations for MMSE receivers can be applied to decorrelation [44]. As the spreading sequences of all K users are linearly independent with probability 1,[5] there are $K-1$ infinite eigenvalues of the covariance matrix of total distortion. The remaining $L-K+1$ eigenvalues are equal to the variance of the AWGN. As the indexing of the eigenvalues is irrelevant, we can set

$$\begin{array}{ccccccccc} \lambda_1 & = & \lambda_2 & = & \cdots & = & \lambda_{K-1} & \to & \infty \\ \lambda_K & = & \lambda_{K+1} & = & \cdots & = & \lambda_L & = & N \end{array} \tag{27}$$

without loss of generality. With (26) and the eigenvalues given in (27), the SNR after decorrelation results in

$$\gamma_{\mathrm{dec}} = \frac{1}{N} \cdot \frac{c_1^2}{c_1^2 + c_2^2} \tag{28}$$

with the definitions

$$c_1^2 \triangleq \sum_{i=K}^{L} |g_i|^2$$

and

$$c_2^2 \triangleq \sum_{i=1}^{K-1} |g_i|^2.$$

As stated in [46] c_1^2 is a χ^2-distributed random variable with $2(L-K+1)$ degrees of freedom. Further, the random variable c_2^2 is also χ^2-distributed, but with $2K-2$ degrees of freedom. With [47, p. 515] or [48, Sec. 26.5] the pdf of the decorrelator's SNR is then found to equal the result given in (4). □

Appendix B
Proof of Proposition 2

For the average channel capacity we use the pdf of SNR after decorrelation given by (4) and the calculus of partial integration to get

$$\begin{aligned} \overline{C}_{\mathrm{dec}} &\triangleq \underset{\boldsymbol{S}}{E}\{\log_2(1+\gamma_{\mathrm{dec}})\} \\ &= \int_{-\infty}^{+\infty} \log_2(1+y) p_{\gamma_{\mathrm{dec}}}(y)\, dy \\ &= \int_0^1 \log_2\left(1+\frac{y}{N}\right) \frac{y^{L-K}(1-y)^{K-2}\, dy}{B(L-K+1,\,K-1)} \\ &= \log_2\left(1+\frac{1}{N}\right) \int_0^1 \frac{y^{L-K}(1-y)^{K-2} dy}{B(L-K+1, K-1)} \\ &\quad - \log_2(e) \int_0^1 \frac{\int_0^y x^{L-K}(1-x)^{K-2}\, dx\, dy}{N\left(1+\frac{y}{N}\right) B(L-K+1,\,K-1)} \end{aligned} \tag{29}$$

[5]As all the following considerations hold only with probability 1, it is not explicitly mentioned further on.

$$\begin{aligned} &= \log_2\left(1+\frac{1}{N}\right) \\ &\quad - \log_2(e) \int_0^1 \frac{B(L-K+1;\,K-1;\,y)\, dy}{N\left(1+\frac{y}{N}\right) B(L-K+1,\,K-1)} \end{aligned}$$

where $B(a;\,b;\,y)$ denotes the incomplete beta function, see, e.g., [18, Ch. 58] for explicit and (29) for implicit definition, respectively. The integral in (29) is studied in more detail in the following. With [18, eq. 58.12.1], [49, eq. 7.512.9],[6] and [35, eq. 1.511] we get

$$\begin{aligned} &I(K,\,L,\,N) \\ &\quad \triangleq \int_0^1 \frac{B(L-K+1;\,K-1;\,y)\, dy}{N\left(1+\frac{y}{N}\right) B(L-K+1,\,K-1)} \\ &\quad = \int_0^1 \frac{y_2^{L-K+1} F_1(L-K+1,\,2-K;\,L-K+2;\,y)}{(L-K+1)N\left(1+\frac{y}{N}\right) B(L-K+1,\,K-1)}\, dy \\ &\quad = \frac{\Gamma(L-K+2)\Gamma(K)\,{}_3F_2\left(1,\,1,\,K;\,2,\,L+1;\,\frac{1}{1+N}\right)}{(L-K+1)\Gamma(L+1)B(L-K+1,\,K-1)(1+N)} \\ &\quad = \frac{K-1}{L(1+N)}\,{}_3F_2\left(1,\,1,\,K;\,2,\,L+1;\,\frac{1}{1+N}\right) \\ &\quad = \frac{K-1}{L(1+N)} \sum_{i=0}^{\infty} \frac{(1)_i (K)_i}{(2)_i (L+1)_i} \left(\frac{1}{1+N}\right)^i \end{aligned}$$

where ${}_3F_2(\cdot,\,\cdot\cdot,\,\cdots;\,\cdots\cdot,\,\cdots\cdot\cdot;\,x)$ denotes the hypergeometric function with three numerator and two denominator parameters. Using the definition of the Pochhammer polynominals, see (7), we get by simple change of the summation index and resubstitution into (29)

$$\overline{C}_{\mathrm{dec}} = \log_2\left(1+\frac{1}{N}\right) - \log_2(e) \sum_{i=1}^{\infty} \frac{(K-1)_i}{i(L)_i} \left(\frac{1}{1+N}\right)^i \tag{30}$$

which is equivalent to (10). This proves the first part of Proposition 2.

The second part of Proposition 2 are an upper and a lower bound on the average capacity. The upper bound simply results from concavity of the logarithm and Jensen's inequality. Thus, only the lower bound remains to be proven. First, we define an auxiliary function

$$f(K,\,L,\,N) \triangleq \sum_{i=1}^{\infty} \frac{1}{i} \left(\frac{K^i}{L^i} - \frac{(K-1)_i}{(L)_i}\right) \left(\frac{1}{1+N}\right)^i. \tag{31}$$

From (30) we get

$$\begin{aligned} \overline{C}_{\mathrm{dec}} &= \log_2\left(1+\frac{1}{N}\right) - \log_2(e) \sum_{i=1}^{\infty} \frac{K^i}{iL^i(1+N)^i} \\ &\quad + \log_2(e) f(K,\,L,\,N) \\ &= \log_2\left(1+\frac{1}{N}\right) + \log_2\left(1-\frac{K}{L(1+N)}\right) \\ &\quad + \log_2(e) f(K,\,L,\,N) \\ &= \log_2\left(1+\frac{L-K}{LN}\right) + \log_2(e) f(K,\,L,\,N) \end{aligned} \tag{32}$$

[6]Reference [35, eq. 7.512.9] describing the same integral is erroneous.

with [35, eq. 1.511], [18, eq. 18.5.6], and the auxiliary function defined in (31). Thus, it remains to be shown that $f(K, L, N) > 0$. For this purpose, we make use of some properties of the sequence

$$s[i] \triangleq \frac{1}{i} \begin{cases} \frac{K^i}{L^i} - \frac{(K-1)_i}{(L)_i}, & i > 0 \\ 0, & i \le 0. \end{cases}$$

In the following we distinguish two cases. The first case assumes that $s[i] \ge 0, \forall i$. In this case, $f(K, L, N) > 0$ holds by definition. The second case assumes that there is an integer i with $s[i] < 0$. Here, a more sophisticated procedure than in the first case is required to show the desired result. First, we prove the following lemma.

Lemma 1: For $1 < K < L$

$$s[i^+] \ge 0 > s[i^+ + 1] \Longrightarrow s[i^+ - \nu] \ge 0 > s[i^+ + \nu] \quad \forall \nu > 0.$$

Proof: The proof aims to show that the opposite to Lemma 1 yields a contradiction. Note that

$$s[i^+] \ge 0 > s[i^+ + 1] \Longrightarrow (i^+ + 1)s[i^+ + 1] - i^+ s[i^+] \frac{K}{L} < 0.$$

With the definition of the sequence $s[\cdot]$ we get

$$\left(\frac{K}{L}\right)^{i^+ + 1} - \left(\frac{K}{L}\right)^{i^+} \frac{K}{L} - \frac{(K-1)_{i^+ + 1}}{(L)_{i^+ + 1}} + \frac{K(K-1)_{i^+}}{L(L)_{i^+}} < 0$$

yielding

$$i^+ > \frac{L}{L-K}.$$

Now, let us assume there is an integer $i_1 > i^+$ with $s[i_1] \ge 0$ which is in contrast to the lemma to be proven. Then, there has to exist an integer $i^- > i^+$ where the sign of the sequence switches, i.e., $s[i^-] < 0 \le s[i^- + 1]$. This implies

$$(i^- + 1)s[i^- + 1] - i^- s[i^-] \frac{K}{L} > 0 \Longrightarrow i^- < \frac{L}{L-K}$$

which is in contrast to $i^+ \le i^-$. Thus, $s[i^+ + \nu] < 0$ holds for all positive integers ν. Up to now, we have shown the following: if the sign of the sequence switches from nonnegative to negative at i^+ it cannot switch again at any integer larger than i^+. As $s[1] = 1/L > 0$ and $s[i^+] \ge 0$, switches in the sign of the sequence $s[\cdot]$ within $1 \le n \le n^+$ are prohibited. Thus

$$s[i^+ - \nu] \ge 0, \forall \nu > 0.$$

This was to be shown. ∎

Lemma 1 shows that there exists an $i^+ > 0$ such that $s[i] > 0$, $\forall i < i^+$, and $s[i] \le 0 \forall i \ge i^+$. This enables us to write (31) by

$$f'(K, L, N) \triangleq f(K, L, N) \left(\frac{1}{1+N}\right)^{-i^+} = \sum_{i=1}^{\infty} x^{1-i} s[i^+ + 1 - i] + s[i^+ + i] x^i$$

with $x \triangleq 1/(1+N) < 1$. No term of the sum increases with increasing x. Thus, we obtain the following lower bound by letting $x = 1$, as x is upper-bounded by 1:

$$f'(K, L, N) > \sum_{i=1}^{\infty} s[i^+ + 1 - i] + s[i^+ + i].$$

Resubstitution of $s[\cdot]$ and the Taylor series of the logarithm yield

$$\begin{aligned} f'(K, L, N) &> \sum_{i=1}^{\infty} \frac{1}{i} \left(\frac{K^i}{L^i} - \frac{(K-1)_i}{(L)_i} \right) \\ &= \frac{K-1}{L} \sum_{i=0}^{\infty} \frac{(1)_i (K)_i}{(2)_i (L+1)_i} + \ln \frac{L}{L-K} \\ &= \psi(L-K+1) - \psi(L) + \ln \frac{L}{L-K} \\ &= \int_{L-K}^{L} \frac{dx}{x} - \sum_{i=L-K+1}^{L-1} \frac{1}{i} > 0 \end{aligned} \tag{33}$$

using some properties of the digamma function $\psi(\cdot)$, see, e.g., [18, Ch. 44]

$$\psi(y) \triangleq \lim_{\ell \to \infty} \left\{ \ln(\ell) - \sum_{i=0}^{\ell} \frac{1}{i+y} \right\}.$$

Obviously, (33) shows that $f'(K, L, N) > 0$ which also implies $f(K, L, N) > 0$. This finally yields

$$\overline{C}_{\text{dec}} > \log_2 \left(1 + \frac{L-K}{LN}\right)$$

with (32) and completes the proof. □

Appendix C
Proof of Proposition 3

Due to spherical symmetry and perfect power control, the kth user's signature sequence is chosen to be $\boldsymbol{s}_k = [1, 0, \ldots, 0]^T$ without loss of generality while the other users' sequences remain random. Then, the sum of squared correlation coefficients becomes

$$\sum_{i \ne k} (\boldsymbol{S}^H \boldsymbol{S})_{ki}^2 = \sum_{i \ne k} \frac{|g_{1i}|^2}{\sum_{\ell=1}^{L} |g_{\ell i}|^2}$$

with (1), where the g_{ik} are independent and identically distributed (i.i.d.) zero-mean complex Gaussian random variables. Let the interference power of user $i \ne k$ be defined as

$$I_i \triangleq \frac{|g_{1i}|^2}{\sum_{\ell=1}^{L} |g_{\ell i}|^2} \qquad \forall i \ne k. \tag{34}$$

Then, the various interference powers are statistically independent, as they are functions of disjoint sets of independent random variables. Recovering the considerations in Appendix A, the similarities of (34) and (28) yield that the interference powers follow beta distributions with identical pdfs

$$p_I(y) = \begin{cases} (L-1)(1-y)^{L-2}, & \text{for } 0 < y < 1 \\ 0, & \text{elsewhere.} \end{cases}$$

The corresponding characteristic function

$$\Phi_I(j\omega) \triangleq \underset{I}{E} \{e^{j\omega I}\} = (L-1) \int_0^1 (1-y)^{L-2} e^{j\omega y} \, dy$$

becomes

$$\Phi_I(j\omega) = (L-1)! \, e^{j\omega} \gamma^*(L-1, j\omega) \tag{35}$$

with [18, eq. 45.3.4].

It will be helpful in the following to define an auxiliary variable

$$\Upsilon_k \triangleq N + \sum_{i \ne k} I_i. \tag{36}$$

By symmetry, average capacities are identical for all users. Thus, the user index is dropped for the following considerations. Then, the average channel capacity can be expressed as

$$\begin{aligned}\overline{C}_{\mathrm{con}} &= \underset{\Upsilon}{E}\left\{\log_2\left(1+\frac{1}{\Upsilon}\right)\right\}\\ &= \int_0^\infty \log_2\left(1+\frac{1}{y}\right) p_\Upsilon(y)\,dy\\ &= \underbrace{\lim_{y\to\infty}\log_2\left(1+\frac{1}{y}\right)P_\Upsilon(y)}_{=0} - \underbrace{\lim_{y\to 0}\log_2\left(1+\frac{1}{y}\right)P_\Upsilon(y)}_{=0}\\ &\quad +\log_2(e)\int_0^\infty \frac{P_\Upsilon(y)}{y(1+y)}\,dy\\ &= \log_2(e)\int_0^\infty \frac{P_\Upsilon(y)}{y}\,dy - \log_2(e)\int_0^\infty \frac{P_\Upsilon(y)}{1+y}\,dy\\ &= -\pi\log_2(e)\lim_{y\to 0}\mathcal{H}\{P_\Upsilon(y)\}\\ &\quad -\log_2(e)\int_1^\infty \frac{P_\Upsilon(y-1)}{y}\,dy\\ &= -\pi\log_2(e)\lim_{y\to 0}\mathcal{H}\{P_\Upsilon(y)-P_\Upsilon(y-1)\}\end{aligned}$$

via integration by parts, decomposition into partial fractions, introduction of Hilbert transform

$$\mathcal{H}\{f(x)\} \triangleq PV\,\frac{1}{\pi}\int_{-\infty}^{+\infty}\frac{f(y)\,dy}{x-y}$$

and change of variables, respectively.

With (36), [50, eq. 5.64], statistical independence of the interference powers, and [50, eq. 7.31] (convolutional theorem), the characteristic function of the auxiliary variable is given by

$$\Phi_\Upsilon(j\omega) = (\Phi_I(j\omega))^{K-1}e^{j\omega N}.$$

With the characteristic functions and the Fourier transform pairs

$$\begin{aligned}P_\Upsilon(y)-P_\Upsilon(y-1) \quad &\circ\!\!-\!\!\bullet \quad \frac{\Phi_\Upsilon(-j\omega)(1-e^{-j\omega})}{j\omega}\\ \mathcal{H}\{\cdot\} \quad &\circ\!\!-\!\!\bullet \quad -j\mathrm{sign}(\omega)\cdot\end{aligned}$$

the average capacity becomes

$$\overline{C}_{\mathrm{con}} = \frac{\log_2 e}{2}\int_{-\infty}^{+\infty}\frac{\Phi_\Upsilon(-j\omega)\,(1-e^{-j\omega})}{\omega}\mathrm{sign}(\omega)\,d\omega.$$

As the difference of the pdfs $p_\Upsilon(y) - p_\Upsilon(y-1)$ is real-valued, the real and imaginary parts of its Fourier transform $\Phi_\Upsilon(-j\omega)\,(1-e^{-j\omega})$ are even and odd functions, respectively. As the odd part vanishes by integration, we get

$$\begin{aligned}\overline{C}_{\mathrm{con}} &= \log_2(e)\int_0^\infty \Re\left\{\Phi_\Upsilon(-j\omega)\,(1-e^{-j\omega})\right\}\frac{d\omega}{\omega}\\ &= \log_2(e)\int_0^\infty \Re\left\{(\Phi_I(-j\omega))^{K-1}e^{-j\omega N}(1-e^{-j\omega})\right\}\frac{d\omega}{\omega}\end{aligned}$$

which becomes equivalent to (15) after inserting (35) and completes the first part of the proof.

The lower bound on average capacity given by (16) directly follows from convexity of the function $x \mapsto \log_2(1+1/x)$ and Jensen's inequality, as

$$\underset{\Upsilon}{E}\{\Upsilon\} = N + (K-1)\,\underset{I}{E}\{I\} = N + \frac{K-1}{L}.$$

Thus, the lower bound has also been shown. □

APPENDIX D
PROOF OF PROPOSITION 4

We have

$$\begin{aligned}\overline{C}_{\mathrm{decDF1}} &= \frac{1}{K}\sum_{k=1}^{K}\overline{C}_{\mathrm{dec}}(k,\,L,\,N)\\ &= \log_2\left(1+\frac{1}{N}\right)\\ &\quad -\frac{\log_2 e}{K}\sum_{k=1}^{K}\sum_{i=1}^{\infty}\frac{(k-1)_i}{i(L)_i}\left(\frac{1}{1+N}\right)^i\\ &= \log_2\left(1+\frac{1}{N}\right)\\ &\quad -\frac{\log_2 e}{K}\sum_{i=1}^{\infty}\frac{(K-1)_{i+1}}{i(i+1)(L)_i}\left(\frac{1}{1+N}\right)^i \qquad (37)\end{aligned}$$

with [51, Sec. III.1D, eq. 14]. Using properties of the Pochhammer polynomials, see (7), we finally obtain

$$\begin{aligned}\overline{C}_{\mathrm{decDF1}} &= \log_2\left(1+\frac{1}{N}\right) - \log_2(e)\,\frac{K-1}{K}\\ &\quad \cdot\sum_{i=1}^{\infty}\frac{(K)_i}{i(i+1)(L)_i}\left(\frac{1}{1+N}\right)^i. \qquad (38)\end{aligned}$$

This proves the first part of Proposition 4. Before addressing the second part of the theorem, the following lemma is proven.

Lemma 2: For the average capacities given in Propositions 2 and 4, the following interrelationship holds:

$$\begin{aligned}&\overline{C}_{\mathrm{decDF1}}(K,\,L,\,N) - \log_2\left(1+\frac{1}{N}\right)\\ &\quad = \frac{K-1}{K}\,(1+N)\int_0^{\frac{1}{1+N}}\overline{C}_{\mathrm{dec}}(K+1,\,L,\,y)\\ &\qquad -\log_2\left(1+\frac{1}{y}\right)\,d\left(\frac{1}{1+y}\right) \qquad (39)\end{aligned}$$

Proof: Inserting (10) into the right-hand side of (39) and performing the calculus of integration, one can verify the validity of Lemma 2 with (38). ■

In order to show that the bounds given in Proposition 4 hold, we take the bounds from Proposition 2 holding for the decorrelator and apply Lemma 2 to obtain bounds for the decorrelating decision-feedback detector. This procedure is justified as Lemma 2 describes a linear functional relationship. This can hardly be seen from Lemma 2 itself, but becomes obvious by looking at (37).

From Proposition 2, we have

$$\begin{aligned}\overline{C}_{\mathrm{dec}} &< \log_2\left(1+\frac{L-K}{NL}\right)\\ &= \log_2\left(1+\frac{1}{N}\right) + \log_2\left(1-\frac{K}{L(1+N)}\right).\end{aligned}$$

Lemma 2 yields by changing variables

$$\begin{aligned}\overline{C}_{\text{decDF1}} &- \log_2\left(1+\frac{1}{N}\right)\\ &< \frac{K-1}{K}(1+N)\int_0^{\frac{1}{1+N}} \log_2\left(1-\frac{K}{L}x\right)dx\\ &= \frac{K-1}{K}\log_2\left(1-\frac{K}{L(1+N)}\right)\left(1-\frac{L(1+N)}{K}\right)\\ &\quad -\frac{K-1}{K}\log_2 e\end{aligned}$$

and completes the proof of the upper bound on capacity. The procedure to prove the lower bound is essentially identical and omitted here. □

ACKNOWLEDGMENT

The author wishes to thank P. Schramm, J. Huber, S. Verdú, S. Shamai, A. Lampe, S. Müller-Weinfurtner, S. Kishore, S. Koschny, and the anonymous reviewers for valuable discussions and help leading to improvement of both quality and presentation of this work.

REFERENCES

[1] U. Madhow and M. L. Honig, "MMSE detection of CDMA signals: Analysis for random signature sequences," in *Proc. IEEE Int. Symp. Information Theory*, San Antonio, TX, Jan. 1993, p. 49.

[2] ——, "On the average near–far resistance for MMSE detection of direct sequence CDMA signals with random spreading," *IEEE Trans. Inform. Theory*, vol. 45, pp. 2039–2045, Sept. 1999.

[3] A. J. Grant and P. D. Alexander, "Randomly selected spreading sequences for coded CDMA," in *Proc. IEEE ISSSTA*, Mainz, Germany, Sept. 1996, pp. 54–57.

[4] ——, "Random sequence multisets for synchronous code-division multiple-access channels," *IEEE Trans. Inform. Theory*, vol. 44, pp. 2832–2836, Nov. 1998.

[5] R. R. Müller, P. Schramm, and J. B. Huber, "Spectral efficiency of CDMA systems with linear interference suppression" (in German), in *Proc. IEEE WSKT*, Ulm, Germany, Jan. 1997, ITUU Tech. Rep. 1997/01, pp. 93–97.

[6] S. Verdú and S. Shamai (Shitz), "Multiuser detection with random spreading and error-correction codes: Fundamental limits," in *Proc. 35th Annu. Allerton Conf. Communication, Control, and Computing*, Monticello, IL, Sept./Oct. 1997, pp. 470–482.

[7] ——, "Spectral efficiency of CDMA with random spreading," *IEEE Trans. Inform. Theory*, vol. 45, pp. 622–640, Mar. 1999.

[8] D. Tse and S. Hanly, "Multiuser demodulation: Effective interference, effective bandwidth and capacity," in *Proc. Annu. Allerton Conf. on Comm., Control, and Comp.*, Monticello, IL, Sep./Oct. 1997, pp. 281–290.

[9] ——, "Linear multiuser receivers: Effective interference, effective bandwidth and user capacity," *IEEE Trans. Inform. Theory*, vol. 45, pp. 641–657, Mar. 1999.

[10] S. Verdú, *Multiuser Detection*. New York: Cambridge Univ. Press, 1998.

[11] J. H. Winters, J. Salz, and R. D. Gitlin, "The impact of antenna diversity on the capacity of wireless communication systems," *IEEE Trans. Commun.*, vol. 42, pp. 1740–1751, Feb./Mar./Apr. 1994.

[12] I. E. Telatar, "Capacity of multi-antenna Gaussian channels," unpublished, June 1995.

[13] T. M. Cover and J. A. Thomas, *Elements of Information Theory*. New York: Wiley, 1991.

[14] A. J. Viterbi, *CDMA*. Reading, MA: Addison-Wesley, 1995.

[15] A. G. Burr, "Performance of linear separation of CDMA signals with FEC coding," in *Proc. IEEE Int. Symp. Information Theory*, Ulm, Germany, June/July 1997, p. 354.

[16] B. R. Vojcic, "Information theoretic aspects of multiuser detection," in *Proc. IRSS*, Washington, DC, Mar. 1997.

[17] M. L. Honig and W. Veerakachen, "Performance variability of linear multiuser detection for DS-CDMA," in *Proc. IEEE Vehicular Technology Conf.*, Atlanta, GA, Apr. 1996, pp. 372–376.

[18] J. Spanier and K. B. Oldham, *An Atlas of Functions*. Berlin, Germany: Springer-Verlag, 1987.

[19] G. R. Cooper and R. W. Nettleton, "A spread-spectrum technique for high-capacity mobile radio," *IEEE Trans. Veh. Technol.*, vol. VT-27, pp. 264–275, Nov. 1978.

[20] O.-C. Yue, "Spread spectrum mobile radio, 1977–1982," *IEEE Trans. Veh. Technol.*, vol. VT-32, pp. 98–105, Feb. 1983.

[21] J. Y. N. Hui, "Throughput analysis for code division multiple accessing of the spread spectrum channel," *IEEE J. Select. Areas Commun.*, vol. SAC-2, pp. 482–486, July 1984.

[22] A. J. Viterbi, "When not to spread spectrum—A sequel," *IEEE Commun. Mag.*, vol. 23, pp. 12–17, Apr. 1985.

[23] ——, "Very low rate convolutional codes for maximum theoretical performance of spread-spectrum multiple-access channels," *IEEE J. Select. Areas Commun.*, vol. 8, pp. 641–649, May 1990.

[24] M. Bickel, W. Granzow, and P. Schramm, "Optimization of code rate and spreading factor for direct-sequence CDMA systems," in *Proc. IEEE ISSSTA*, Mainz, Germany, Sept. 1996, pp. 585–589.

[25] S. Shamai (Shitz) and S. Verdú, "Worst case power-constraint noise for binary-input channels," *IEEE Trans. Inform. Theory*, vol. 38, pp. 1494–1511, Sept. 1992.

[26] M. B. Pursley, "Performance evaluation for phase-coded spread-spectrum multiple-access communication—Part I: System analysis," *IEEE Trans. Commun.*, vol. COM-25, pp. 795–799, Aug. 1977.

[27] C. C. Chan and S. V. Hanly, "The capacity improvement of an integrated successive decoding and power control scheme," in *Proc. IEEE ICUPC*, San Diego, CA, Oct. 1997, pp. 800–804.

[28] R. R. Müller and J. B. Huber, "Capacity of cellular CDMA systems applying interference cancellation and channel coding," in *Proc. CTMC at IEEE GLOBECOM*, Phoenix, AZ, Nov. 1997, pp. 179–184.

[29] D. Warrier and U. Madhow, "On the capacity of cellular CDMA with controlled power disparities," in *Proc. IEEE Vehicular Technology Conf.*, Ottawa, ON, Canada, May 1998, pp. 1873–1877.

[30] A. Lampe, R. R. Müller, and J. B. Huber, "Multi-cellular CDMA systems with interference cancellation: Effects of path loss, shadowing and handover strategies," in *Proc. IEEE GLOBECOM*, Sydney, Australia, Nov. 1998, pp. 1888–1893.

[31] R. Price, "Nonlinear feedback equalized PAM versus capacity for noisy filter channels," in *Proc. IEEE Int. Communications Conf.*, Philadelphia, PA, June 1972, pp. 22.12–22.17.

[32] M. V. Eyuboğlu, "Detection of coded modulation signals on linear severely distorted channels using decision-feedback noise prediction with interleaving," *IEEE Trans. Commun.*, vol. 36, pp. 401–409, Apr. 1988.

[33] J. W. Silverstein and Z. D. Bai, "On the empirical distribution of eigenvalues of a class of large dimensional random matrices," *J. Multivariate Anal.*, vol. 54, pp. 175–192, 1995.

[34] L. Pastur, "Eigenvalue distributions of random matrices: Some recent results," *Ann. Inst. Henri Poincaré Phys. Theor.*, vol. 64, no. 3, pp. 325–337, 1996.

[35] I. S. Gradshteyn and I. M. Ryzhik, *Table of Integrals, Series, and Products*, 4th ed. New York: Academic, 1965.

[36] P. Schramm and R. R. Müller, "Spectral efficiency of CDMA systems with linear MMSE interference suppression," *IEEE Trans. Commun.*, vol. 47, pp. 722–731, May 1999.

[37] M. K. Varanasi and T. Guess, "Optimum decision feedback multiuser equalization with successive decoding achieves the total capacity of the Gaussian multiple-access channel," in *Proc. Asilomar Conf. Signals, Systems, and Computing*, Monterey, CA, Nov. 1997, pp. 1405–1409.

[38] J. M. Cioffi, G. P. Dudevoir, M. V. Eyuboğlu, and G. D. Forney, "MMSE decision-feedback equalizers and coding—Part I: Equalization results," *IEEE Trans. Commun.*, vol. 43, pp. 2582–2594, Oct. 1995.

[39] ——, "MMSE decision-feedback equalizers and coding—Part II: Coding results," *IEEE Trans. Commun.*, vol. 43, pp. 2595–2604, Oct. 1995.

[40] S. Shamai (Shitz) and R. Laroia, "The intersymbol interference channel: Lower bounds on capacity and channel precoding loss," *IEEE Trans. Inform. Theory*, vol. 42, pp. 1388–1404, Sept. 1996.

[41] S. Verdú, "Capacity region of Gaussian CDMA channels: The symbol-synchronous case," in *Proc. 24th Annu. Allerton Conf. Communication, Control, and Computing*, Monticello, IL, Oct. 1986, pp. 1025–1034.

[42] B. Rimoldi and R. Urbanke, "A rate-splitting approach to the Gaussian multiple-access channel," *IEEE Trans. Inform. Theory*, vol. 42, pp. 364–375, Mar. 1996.
[43] A. Lampe, R. R. Müller, and J. B. Huber, "Transmit power allocation for Gaussian multiple access channels with diversity," in *Proc. IEEE International Theory Workshop*, Kruger National Park, South Africa, June 1999, p. 101.
[44] U. Madhow and M. L. Honig, "MMSE interference suppression for direct-sequence spread-spectrum CDMA," *IEEE Trans. Commun.*, vol. 42, pp. 3178–3188, Dec. 1994.
[45] T. L. Marzetta and B. M. Hochwald, "Capacity of a mobile multiple-antenna communication link in Rayleigh flat fading," *IEEE Trans. Inform. Theory*, vol. 45, pp. 139–157, Jan. 1999.
[46] J. G. Proakis, *Digital Communications*, 3rd ed. New York: McGraw-Hill, 1995.
[47] M. Fogiel, *Handbook of Mathematical Formulas, Tables, Functions, Graphs, Transforms*. New York: Res. Educ. Assoc., 1983.
[48] M. Abramowitz and I. Stegun, *Handbook of Mathematical Functions*. New York: Dover, 1965.
[49] I. S. Gradshteyn and I. M. Ryzhik, *Table of Integrals, Series, and Products*. New York: Academic, 1980.
[50] A. Papoulis, *Probability, Random Variables, and Stochastic Processes*, 3rd ed. New York: McGraw-Hill, 1991.
[51] V. Mangulis, *Handbook of Series for Scientists and Engineers*. New York: Academic, 1965.